Nova Acta Científica Compostelana, 30 (2023). ISSN-e: 2340-0021
https://doi.org/10.15304/nacc.id8975

Scientific articles

Anatomical study of *Onchidella celtica* (Gastropoda, Eupulmonata, Onchidiidae) by micro-computed tomography (micro-CT). A first approach to its use in Onchidiidae (Gastropoda, Eupulmonata)

Estudio anatómico de *Onchidella celtica* (Gastropoda, Eupulmonata, Onchidiidae) mediante microtomografía computarizada (micro-CT). Una primera aproximación a su uso en Onchidiidae (Gastropoda, Eupulmonata)

Jesús Fernández-Gutiérrez[1,2,a], Victoriano Urgorri[1], María Candás[1], Guillermo Díaz-Agras[1]

[1] Estación de Bioloxía Mariña da Graña (REBUSC), Universidade de Santiago de Compostela, rúa da Ribeira 1-4 (A Graña), 15590 Ferrol (Galicia), Spain

[2] Interdisciplinary Centre of Marine and Environmental Research (CIIMAR), University of Porto, Novo Edifício do Terminal de Cruzeiros do Porto de Leixões, Avenida General Norton de Matos, 4450-208 Matosinhos, Portugal

[a] *Corresponding author*: jesus.fernandez.gutierrez@rai.usc.es

Abstract

The family Onchidiidae comprises a group of air-breathing marine slugs that can be very abundant in the intertidal zone of temperate shores worldwide. Recently, the phylogeny of the genus *Onchidella* has been reassessed by means of molecular markers, but anatomical studies are still needed to support these conclusions. In the present work, the anatomy of *Onchidella celtica* has been studied by using X-ray micro-computed tomography (micro-CT), a non-invasive technique that allows for 2D and 3D imaging of the external and internal anatomy of specimens without irreversible damage. To date, the potential of this technique for the anatomical study of onchidiids had not been assessed yet and therefore a reconstruction of the whole internal anatomy of *O. celtica* is provided here. Most of the organs and structures were clearly visualized; our observations largely agree with previous descriptions also highlighting the usefulness of micro-CT for the anatomical study of onchidiids.
Keywords: Onchidiidae, Onchidella celtica, micro-CT, anatomy, Eupulmonata

Resumen

La familia Onchidiidae incluye un grupo de babosas marinas que respiran aire y pueden ser muy abundantes en el intermareal de las costas templadas de todo el mundo. Recientemente, la filogenia del género *Onchidella* ha sido revisada mediante el uso marcadores moleculares, pero se necesitan estudios anatómicos que respalden estas conclusiones. En este trabajo, se estudia la anatomía de *Onchidella celtica* mediante el uso microtomografía computarizada de rayos X (micro-CT), una técnica no invasiva que permite obtener imágenes en 2D y 3D de la anatomía externa e interna de los especímenes sin provocar daños irreversibles. Hasta la fecha, se desconocía el potencial de esta técnica para el estudio anatómico de los miembros de Onchidiidae por lo que se presenta aquí una reconstrucción de toda la anatomía interna de *O. celtica*. En general, se pudo visualizar claramente todos los órganos y estructuras; además, nuestras observaciones coinciden en gran medida con descripciones anteriores y ponen de manifiesto la utilidad del micro-CT para el estudio anatómico de los Onchidiidae.

INTRODUCTION

The family Onchidiidae RAFINESQUE, 1815 includes a group of air-breathing gastropods that lack an internal shell and thus should be considered true slugs, closely related to terrestrial ones (DAYRAT *et al.*, 2011a). With the exception of a few species adapted to upland forests (DAYRAT, 2010), all onchidiids are truly marine and are widespread throughout temperate seas of the world (see GOULDING *et al.*, 2022 for further details on the distribution of each species). They inhabit the upper and middle intertidal zone of rocky, sandy and muddy habitats, including mangroves, where their diversity is the highest (HOFFMANN, 1928; BRITTON, 1984).

Despite its distribution and relative abundance in some ecosystems, the biodiversity of Onchidiidae has been traditionally poorly studied (DAYRAT, 2009), and therefore, "the classification of this group was a troublesome task" (MARCUS, 1979). Until a few years ago, the most "modern" taxonomic revisions of the family were those of PLATE (1893), HOFFMANN (1928) and LABBÉ (1934). Most species were described based on external characters even of preserved slugs and (if so) a few internal ones (i.e., male copulatory organs and/or radular arrangement), often neglecting the whole internal anatomy. Therefore, new species and genus names were wrongly assigned despite the weak distinction between specimens, increasing the number of synonyms within the family (DAYRAT, 2009). As a result, descriptions of onchidiids were frequently not reliable for species identification (GOULDING *et al.*, 2018a; DAYRAT *et al.*, 2019a).

Since DAYRAT (2009), an exhaustive taxonomic revision of the family has been initiated by using both molecular and morphological approaches, describing new taxa, revisiting and clarifying the nomenclatural status of almost all species of Onchidiidae (DAYRAT, 2010; DAYRAT *et al.*, 2017, 2018, 2019a, 2019b, 2019c, 2019d, 2020; DAYRAT & GOULDING, 2017; GOULDING *et al.*, 2018a, 2018b, 2021). GOULDING *et al.* (2022) reconstructed the phylogeny of the family recognising a total of 67 valid onchidiid species worldwide. As a result of this, only 4 out of 17 Atlantic species of *Onchidella* Gray, 1855 (MARCUS, 1979) are actually valid (GOULDING *et al.*, 2022). Nevertheless, this delineation was based mainly on molecular markers and thus, morphological analyses are urged to assess at least inter- and intra-specific variation of anatomical characters (BRITTON, 1984). For instance, this has only been done once with some species of *Onchidella* (DAYRAT *et al.*, 2011b) excluding East-Atlantic species.

In order to study the internal anatomy of onchidiids, classical techniques of dissection and histological section of specimens have been used (see WATSON, 1925; WEISS & WÄGELE, 1998; MANIEI *et al.*, 2020). These labour-intensive techniques usually lead to the destruction of the specimen, which is a problem when few are available (FAULWETTER *et al.*, 2013; CANDÁS *et al.*, 2016). Micro-computed tomography (=computed microtomography, micro-CT) is a non-destructive imaging technique based on the measurement of X-rays attenuation when passing through a sample that rotates on itself (180º or 360º), providing a large number of X-ray projection images. From the latter, 2D virtual sections (similar to histological ones) are obtained in transverse, frontal and sagittal planes, as well as 3D reconstructions that allow the visualization of internal and external structure with no alteration or destruction of the sample (ALBA-TERCEDOR & SÁNCHEZ-TOCINO, 2011; FAULWETTER *et al.*, 2013; CANDÁS *et al.*, 2016; ZIEGLER *et al.*, 2018). This is probably the greatest advantage of micro-CT because the studied specimen is still suitable for further examination by other procedures such as light microscopy, scanning electron microscopy (SEM) and even DNA extraction (FAULWETTER *et al.*, 2013; GIGNAC *et al.*, 2016). Therefore, this also allows for re-examination of type material avoiding further damage (PARAPAR *et al.*, 2017; KEKLIKOGLOU *et al.*, 2019).

According to DAYRAT (2009), type material of onchidiid slugs is sometimes quite limited and, due to the lack of reliability in the specific identification quoted previously, there are

museum lots simply labelled as “Onchidiidae”. The aim of this work is to prove the potential of micro-CT to describe the anatomy of onchidiids. As a first approach, the anatomy of a single species, *Onchidella celtica* (AUDOUIN & MILNE-EDWARDS, 1832), is entirely reconstructed and described in the present paper by using micro-CT. Additionally, external morphology is also described, and the results are compared with previous descriptions.

MATERIAL AND METHODS

Collection

A total of 120 *Onchidella celtica* specimens were collected during a year (October 2020-2021) at Praia de Ancoradoiro (42º 20' 1.520" N; 008º 49' 36.820" W), a moderately exposed rocky shore in southern Galicia (NW Iberian Peninsula). Sampling was carried out monthly *via* reef-walking at low tide. Animals were taken by hand when grazing over the rock surface and non-randomly selected to represent monthly variation in size and colour (GOULDING *et al.*, 2018a). They were measured *in situ* and placed separately in seawater. Some specimens were photographed in their habitat while most of them were photographed in the laboratory. For each specimen, external anatomy was described *in vivo* avoiding the loss of information of those characters that may be altered during fixation (URGORRI *et al.*, 2021).

Anaesthesia, fixation and preservation

Anaesthesia, fixation and preservation of specimens were carried out following URGORRI (1981) and URGORRI *et al.* (2021). First, animals were anaesthetised with 7% MgCl2 diluted in equal parts of freshwater and seawater. After anaesthesia, fixation was performed gradually by dripping Bouin’s liquid (fixative liquid) with a Pasteur pipette. The addition of the fixative liquid was observed under the stereomicroscope preventing any sudden reactions of the specimen. After fixation, animals were embedded in Bouin’s liquid for several days, and then preserved in 70% EtOH.

41 individuals were anaesthetized as described above and the remaining 79 specimens were directly fixed and preserved on 100% EtOH. Each specimen was labelled with a code including location (ANC, "Ancoradoiro"), site (1, 2, 3) and date of collection (dd/mm/yyyy) and specimen number (1 to 10). All this material was deposited on the malacological collection of the Marine Biological Station of A Graña (Ferrol, Spain).

Micro-CT procedures

Study of the anatomy of the specimens was done by means of micro-CT. Two mature adults (ANC110092103 and ANC110092104) were examined to ensure that the reproductive system was fully developed; both specimens were preserved in 70% EtOH, dehydrated in 80%, 90% and 96% EtOH baths each of 12 h.

Two different treatments were further applied before scanning depending on the specimen to determine the presence of subdermal spicules (see below). ANC110092104 was stained with 1% iodine in 96% EtOH for 3 days, then dehydrated with hexamethyldisilazane (HMDS) for 2 h and air dried overnight (ALBA-TERCEDOR & SÁNCHEZ-TOCINO, 2011; FAULWETTER *et al.*, 2013; CANDÁS *et al.*, 2014). Iodine staining was first dispensed with for ANC110092103. Thus, the animal was directly transferred from the 96% EtOH to HMDS for the same time as above.

Nova Acta Científica Compostelana, 30 (2023). ISSN-e: 2340-0021
https://doi.org/10.15304/nacc.id8975

Once scanned, the specimen was stained with iodine, dehydrated like ANC110092104 and scanned again.

The specimens were scanned on a Skyscan 1172 microtomograph (Bruker, Belgium) using the following parameters: 55 kv, 165 µA, no filter and 360º sample rotation. Pixel size were 3.66 µm for ANC110092104 and 4.54 µm and 4.06 µm for ANC110092103 stained and no-stained, respectively.

X-rays projection images were reconstructed with the NRecon software (Bruker, Belgium) obtaining 2D sections that were posteriorly cleaned with the CTAn software (Bruker, Belgium). Frontal, sagittal and transverse sections were visualized using DataViewer software, while three dimensional models were obtained with the CTVox software (Bruker, Belgium). 3D images were reconstructed using the Amira® v.5.4.4 software (Visage Imaging, Richmond, Australia).

RESULTS

External Anatomy

Dorsal notum of living animals generally light or dark grey, occasionally olive green (Figs. 1A,B). Juveniles and immature adults (< 3 mm) whitish, sometimes translucent (Fig. 1C). Pedal sole and hyponotum white or creamy, always in contrast with body dorsal part (Figs. 1C,D). Body oval or round, oblong when crawling. Size between 1-25 mm, reaching largest values in late summer. A slightly reduction in length observed after fixation.

Fig. 1. *Onchidella celtica*. Habitus and external appearance *in vivo*. A: Dorsal view of a dark grey adult ANC207102102. B: Dorsal view of a green olive adult ANC202032101. C: Dorsal view of a whitish juvenile specimen ANC329032106. D: Ventral view of a light grey adult ANC217012102. E: Ventral view of a green olive adult ANC126022102.

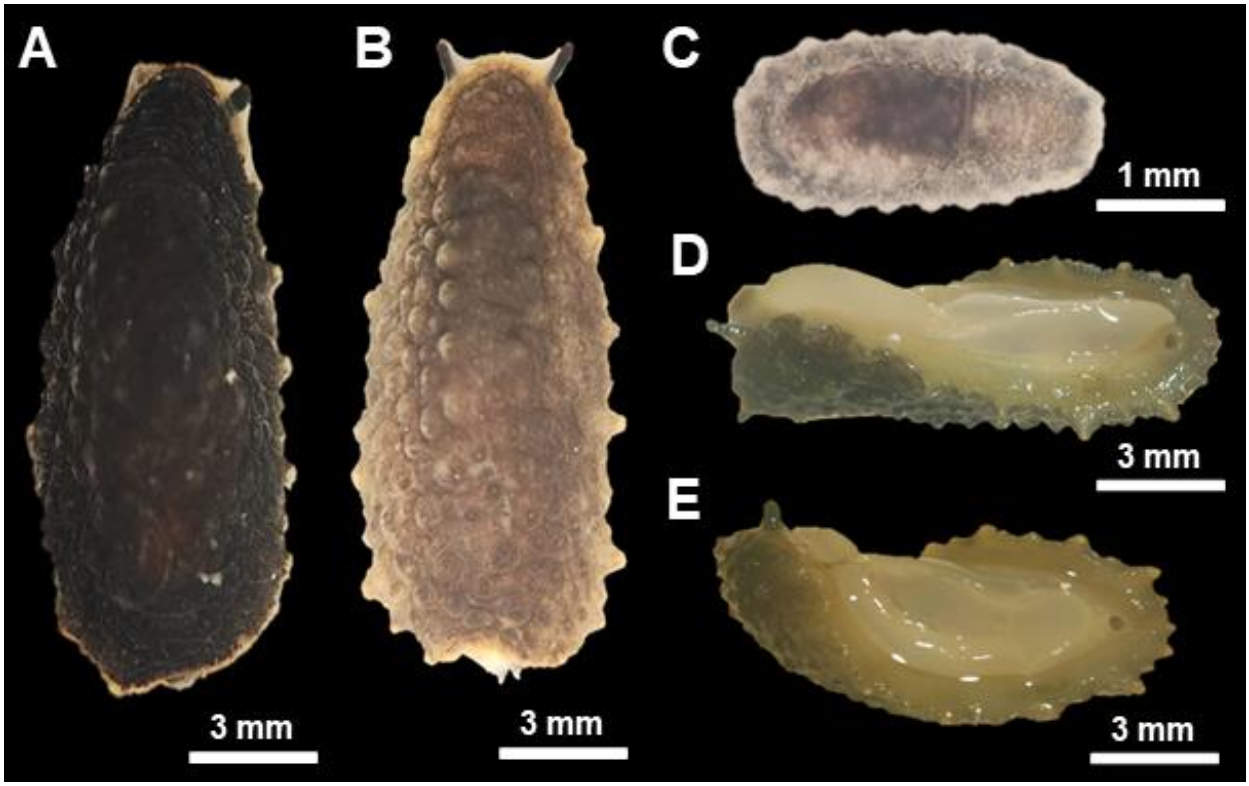

Figure 2. Habitus and external appearance of the scanned specimens. A: Dorsal view of ANC110092104. B: Dorsal view of ANC110092103 stained. C: Dorsal view of ANC110092103 unstained. D: Ventral view of ANC110092104. E: Detail of the cephalic region of ANC110092104. F: Ventral view of ANC110092103 unstained. G: Detail of the caudal region of ANC110092103 stained

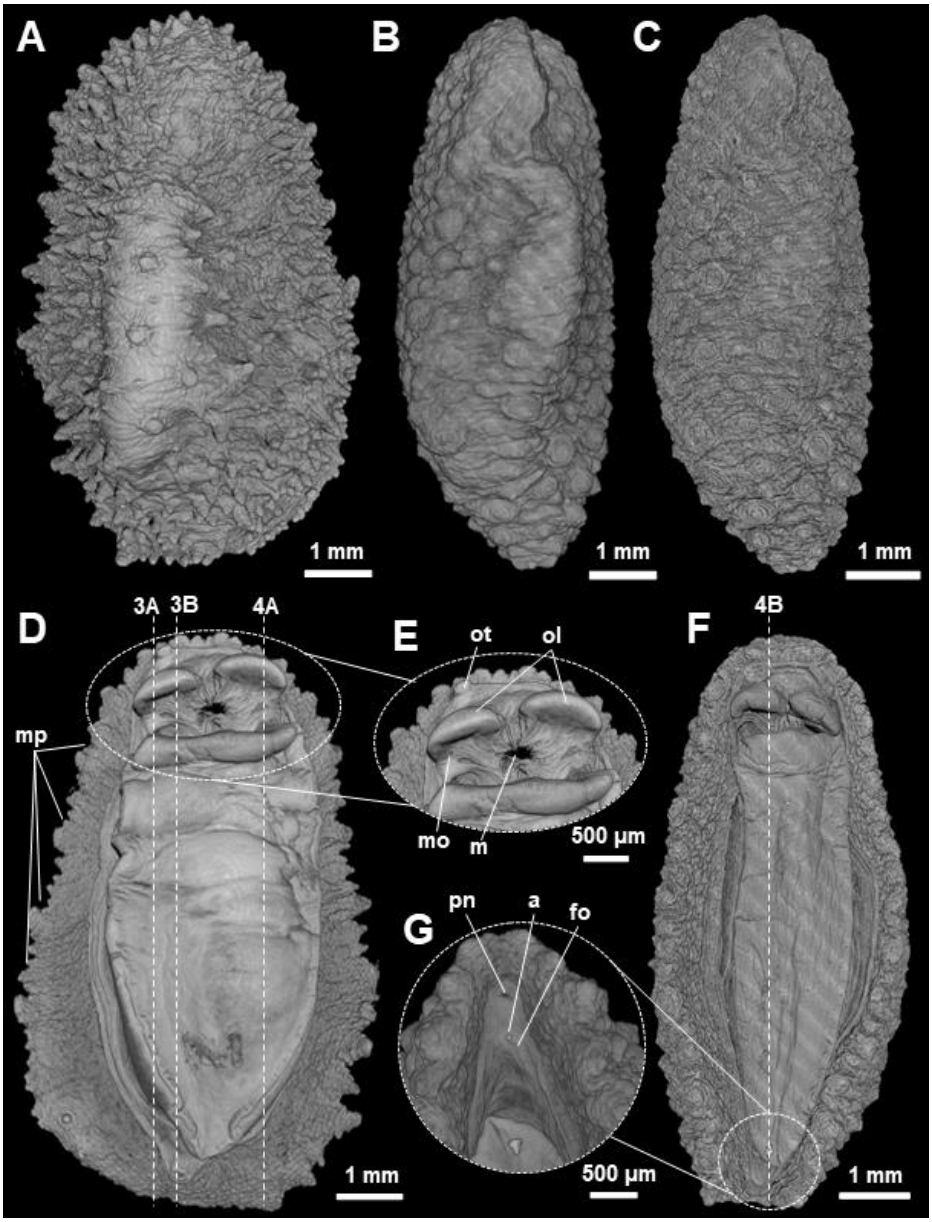

Dorsal surface covered of hemispherical tubercles (=notal/dorsal papillae, pustules, warts) in variable density (Figs. 2A-C) Tubercles more abundant and globular on central notum than on perinotal border, but number fairly constant along dorsal surface. Juveniles and small adults with fewer tubercles showing a smoother notum. Central and anterior notal tubercles bigger than perinotal and posterior ones. Tubercles in living animals switching from hemispherical to conical or pointed when subjected to wind, direct sunlight or dryness. Tubercles in preserved specimens flattened sometimes. Dorsal gills and dorsal eyes not present.

Notum laterals uneven. Larger tubercles (=marginal papillae) surrounded by small ones covering perinotal glands. Marginal papillae lighter in colour than on dorsal surface, similar to hyponotum. Posterior papillae generally bigger than anterior ones. Marginal papillae rounded or pyramid-shaped (Fig. 2C), sometimes indistinguishable in juveniles.

Nova Acta Científica Compostelana, 30 (2023). ISSN-e: 2340-0021
https://doi.org/10.15304/nacc.id8975

Hyponotal border reduced in juveniles but wider than pedal sole in adults completely covering head and foot in disturbed animals. Hyponotal line dividing hyponotum into a granulose outer area (i), broader than a smooth inner one (ii) (close to the foot). Pedal sole (Figs. 2D,F) smooth and similar in colour to hyponotum. Foot ending posteriorly to mouth, close to pedal gland opening. Ciliated groove running along foot right side to caudal region, reaching female genital opening, the latter at right side of anus. Anus caudomedian. Pneumostome present in hyponotal line, always above anus (Fig. 2G).

Cephalic region well defined, bearing two optical tentacles with eyes at tip, retracted in preserved animals (Fig. 2E). Mouth surrounded by a pair of sensorial oral lobes of same size and not fused centrally. Male genital opening on right side of right oral lobe (Fig. 2E).

Internal Anatomy

Subdermal structures and glands

Perinotal glands (=marginal/repulsive glands) in body wall below notum, surrounding visceral cavity (Fig. 5C). 8 pairs of perinotal glands on each side; 9 pairs only in ANC129032101. Perinotal glands pyriform, circular in section. Glandular duct thin, opening distally and leading medially to marginal papillae tip (Fig. 5E). All glands arranged in a single row and almost all in same frontal plane. Posterior perinotal glands located slightly more ventrally. Central perinotal glands wider than anterior and posterior ones.

Figure 3. A-B: Internal anatomy of ANC110092104 from right-sagittal view.

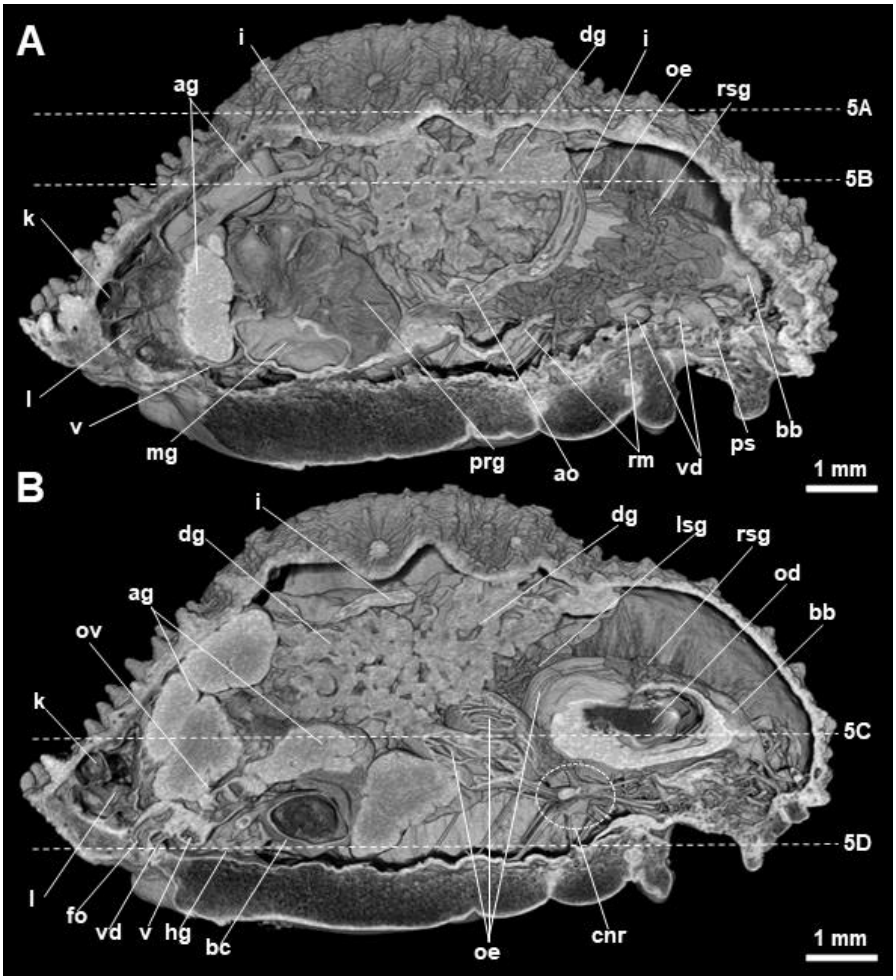

Figure 4. A: Internal anatomy of ANC110092104 from left-sagittal view. B: Internal anatomy of ANC110092103 unstained from left-sagittal view. C: Detail of the cephalic region of ANC110092103 unstained from right-sagittal view. D: Detail of the caudal region of ANC110092104 from left-sagittal view.

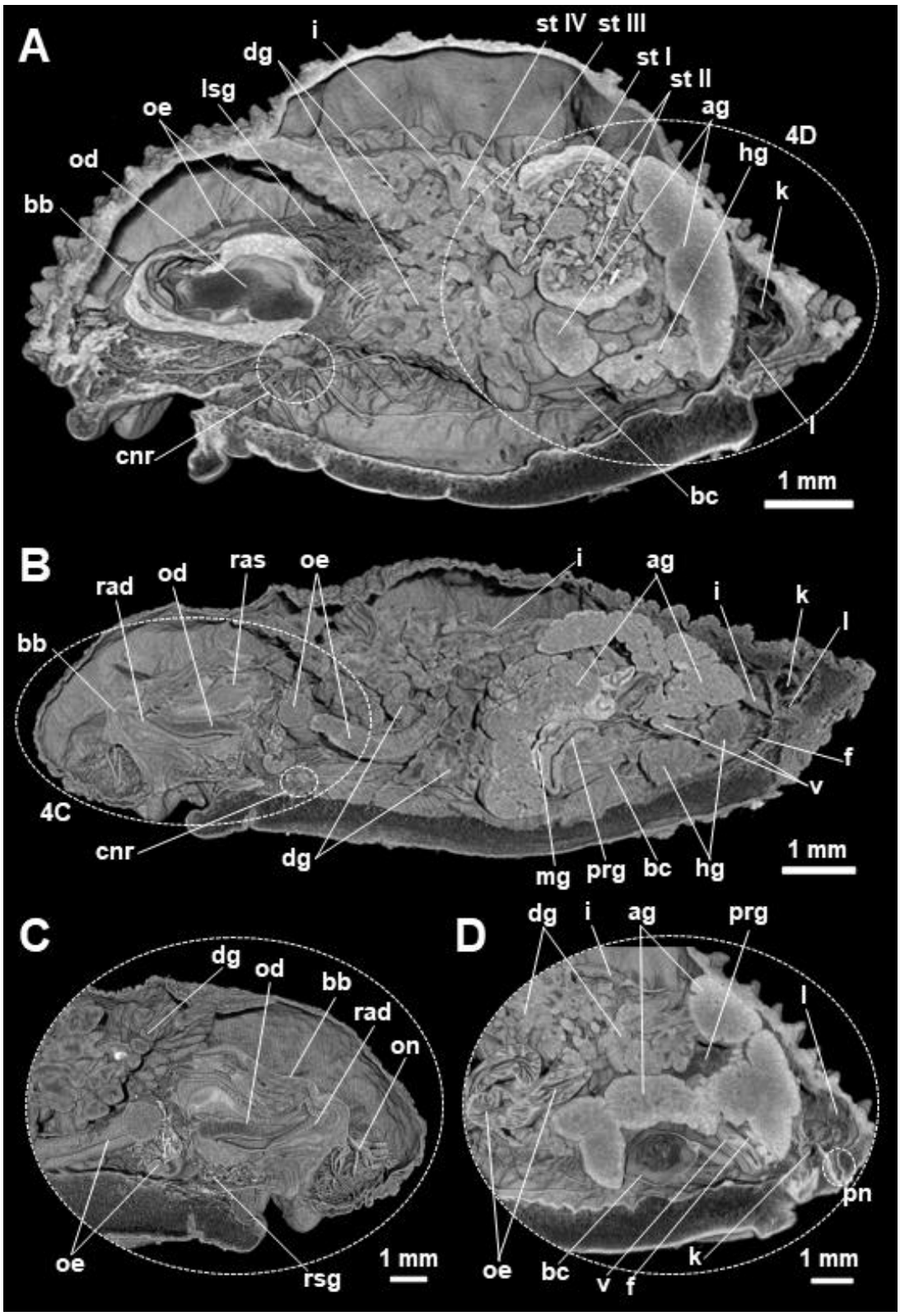

Nova Acta Científica Compostelana, 30 (2023). ISSN-e: 2340-0021
https://doi.org/10.15304/nacc.id8975

Figure 5. Internal anatomy of ANC110092104. A-C: Front-dorsal view. D: Front-ventral view. E: Transverse section of a perinotal gland showing the outlet of the glandular duct at the tip of the marginal papilla.

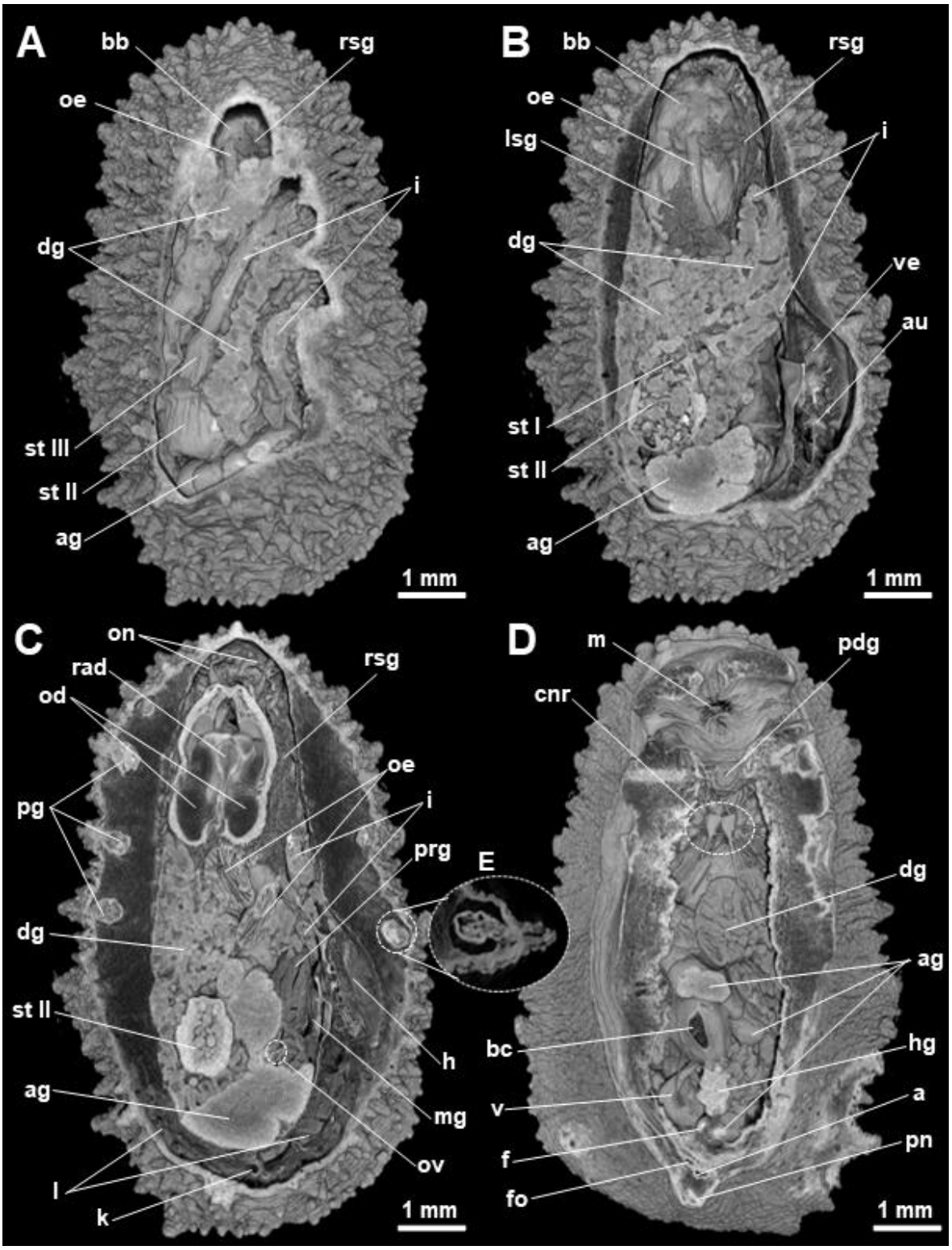

Figure 6. Internal anatomy of ANC110092104 reconstructed with Amira® v.5.4.4 software. A: Dorsal view. B: Ventral view. Central nervous ring containing cerebral ganglia (pink), pleural ganglia (blue), visceral ganglion (green) and pedal ganglia (yellow). (*) showing the end of the penial retractor muscle. C: Right lateral view (digestive and albumen glands transparent for better visualisation). D: Left lateral view (digestive and albumen glands transparent for better visualisation).

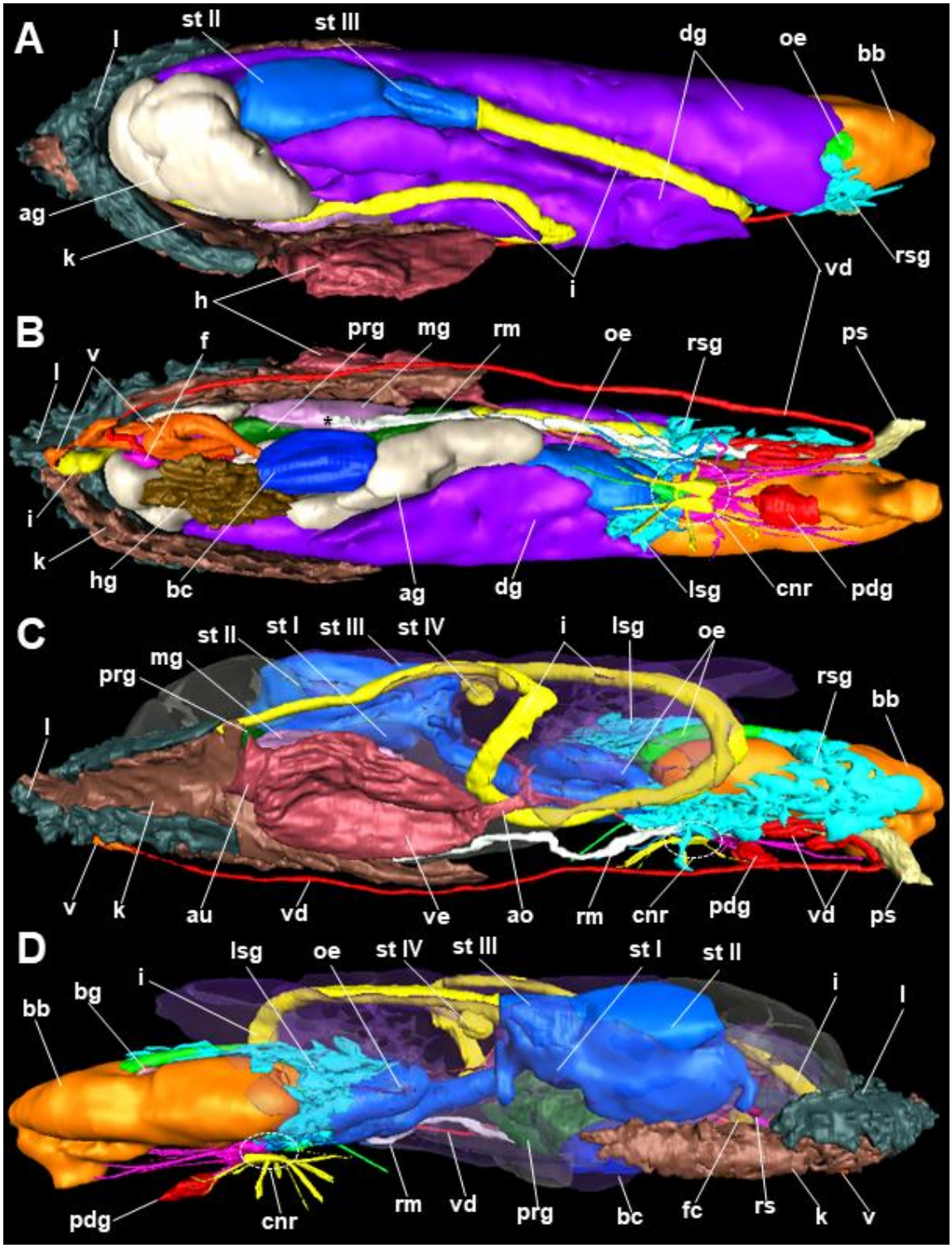

Nova Acta Científica Compostelana, 30 (2023). ISSN-e: 2340-0021
https://doi.org/10.15304/nacc.id8975

Pedal gland located between mouth and anterior foot end (Figs. 5D, 6B-D). Gland one-chambered, rectangular in section. Frontal wall of pedal gland reduced and merging with pedal sole tissue. Secreting pore, subdermal spicules or concretions not observed.

Digestive system

Digestive system occupying most of visceral cavity. Mouth opening between oral lobes and leading to a short oral tube (Figs. 2E, 5D). Frontal wall of oral tube with a thin, inconspicuous and slightly refringent jaw-like structure. Short oral tube entering buccal bulb (=pharynx) mid-ventrally (Figs. 3A,B, 4A-C, 5A,B, 6A,C,D). Buccal bulb conspicuously muscularized, spherical and oblong and subdivided posteriorly into two globous muscular bulbs. Radular sac (=radular papilla) (Fig. 4B) inserted between muscular bulbs and containing radula (Figs. 4B,C, 5C) and odontophore (Figs. 3B, 4A-C, 5C). Teeth and number of rows not distinguishable (radular formula be provided). Odontophore solid, boat-shaped and half-divided at radular sac end.

Left and right salivary glands (Figs. 3A,B, 4A,C, 5A-C, 6A-D) joining buccal mass dorsally near oesophageal aperture. Salivary glands clustered and elongated. Oesophagus (Figs. 3A,B, 4A-C, 5A-C, 6A-D) opening in buccal bulb upper middle area. Oesophageal tube proximal part narrow and surrounding buccal bulb to nerve ring, widening after and then slightly decreasing before entering stomach antero-ventrally.

Stomach subdivided into four parts. Stomach I (Figs. 4A, 6C,D) sac-like at oesophagus end. External walls of initial chamber smooth. Stomach I leading to stomach II (=gizzard) as a bigger oval chamber surrounded by two thick muscular layers (dorsal and ventral) and filled with sand grains (Figs. 4A,B, 5A-C, 6A,C,D), where grinding of food particles occurs. Stomach II opening up anteriorly to a smaller sacculus, stomach III (Figs. 4A, 5A, 6A,C,D), before intestinal aperture. Stomach III walls only distinguishable from stomach II by lacking of muscularized walls. Stomach IV as small sac-like caecum in initial intestine portion (Figs. 4A, 5A, 6A,C,D); epithelium clearly distinct from that of intestine.

Massive digestive gland (Figs. 3A,B, 4A-D, 5A-D, 6A,B) extending over entire dorsal region of visceral cavity and branching into three lobes. Right and left lobes projecting anteriorly, latter longer than other. Third lobe situated postero-ventrally to stomach II and joining dorsally with left branch. Insertion of digestive gland left and right ducts between stomachs I and II. A third duct opening in mid-posterior wall of stomach II and leading to digestive gland caudal lobe.

Intestine (Figs. 3A,B, 4A,B,D, 5A-C, 6A-D) long and narrow. Intestinal duct running first anteriorly, then describing an U-shaped loop (see Fig. 6C) and ending at anus. Intestine diameter lightly variable until terminal portion, where compressed by albumen gland.

Nervous system

Central nerve ring (Figs. 3B, 4A,B, 5D, 6B-D) located before enlargement of oesophageal tube and composed of four types of ganglia. Cerebral ganglia (i) oblong and situated anteriorly. Cerebral ganglia joined dorsally by a thick commissure and ventrally by a thinner one. Four cerebral nerves on each side innervating cephalic region (mouth, buccal bulb, sensorial lobes and eyes). An additional fifth nerve arising from right ganglion innervating male anterior reproductive system.

Pleural ganglia located after cerebral ganglia. Both pairs of ganglia almost fused, connected by a short thin commissure. Pleural ganglia oval and smaller than cerebral ones. Three pairs of pleural nerves at each side innervating mantle cavity walls. Visceral ganglion after pleural ones and connected to these by an elongated commissure. Visceral ganglion

slightly right displaced. Two thick visceral nerves arising from visceral ganglia. One nerve projected to inner body cavity penetrating digestive gland; second nerve bifurcated proximally and innervating respectively aorta and lung plus kidney.

Pedal ganglia conspicuous and oblong. Pedal ganglia joined to cerebral ones below ventral commissure. Thick nerve arising from ventral commissure innervating pedal gland. Two commissures connecting pedal ganglia. Posterior (=parapedal) commissure longer than anterior one. Five nerves arising from left pedal ganglion, only four observed from right one, all innervating pedal sole.

Very small oval buccal ganglia (Fig. 6D) observed outside central nerve ring, above buccal bulb. Buccal ganglia joined by a short and thin commissure below oesophagus. Efferent nerves not observed.

Sensory structures. No statocysts. Oral lobes and eyes densely innervated (see Figs. 4C, 5C).

Circulatory system

Pericardium located on posterior third of body right side, enclosing a two-chambered heart (Figs. 5C, 6A,B). Anterior and large ventricle (Figs. 5B, 6C) situated before a smaller auricle. Auricle posterior wall connecting with renal-pulmonary complex by a fine diaphragm. Ventricle anterior wall opening medially to large aorta projected to visceral mass centre. Aorta (Figs. 3A, 6C) branching anteriorly and posteriorly into cephalic and visceral arteries, respectively. Cephalic artery passing through central nerve ring and then divided in smaller vessels irrigating cephalic and reproductive regions. Visceral artery densely branched irrigating digestive system.

Renal-pulmonary complex

Lung (Figs. 3A,B, 4A,B,D, 5C, 6A-D) in mantle cavity and out of body cavity, located at posterior body end. Lung opening to the air through a very muscularized pneumostome, (Figs. 2G, 4D, 5C) leading to a small canal ending in ample pulmonary cavity (=lung). Lung divided into two branches running laterally towards anterior body and ending at level of heart posterior end. Right branch slightly longer than left. First third of right branch subdivided dorsally and ventrally. Dorsal division connected to pericardium via diaphragm. Respiratory epithelium thin and inconspicuous.

Kidney (Figs. 3A,B, 4A,B,D, 5C, 6A-D) branched similarly to lung. Renal branches joining above pulmonary cavity and running along lung inner side. Ureter at left branch proximal end connecting excretory system with rectum. Left branch oblong, not subdivided and projecting forward aligning with first ventricular third. Right branch longer than left ending at aorta insertion. Right branch compressed against pericardium and only developing ventrally after passing auricle. Renal tissue more conspicuous than pulmonary tissue. Internal epithelium smooth lacking lamellae but occasionally with small folds.

Reproductive system

Reproductive system: posterior parts

Female genital opening (Figs. 2G, 5D) to right side of anus leading to a handle-shaped, narrow vaginal duct (Figs. 3A,B, 4B,D, 5D, 6B-D). Vagina next section much straighter and wider

Nova Acta Científica Compostelana, 30 (2023). ISSN-e: 2340-0021
https://doi.org/10.15304/nacc.id8975

than previous, then bifurcating in a fine, elongated tube and a thicker, shorter one. Flagellum (=vaginal gland) (Figs. 4B,D, 5D, 6B) arising before bifurcation. Flagellum long, coiled, orientated posteriorly, lying on vaginal tube inner wall. Elongated tube projecting into central visceral cavity terminating at a big bursa copulatrix (Figs. 3B, 4B,D, 5D, 6B,D). Bursa copulatrix (=spermatheca) of ANC110092104 filled with sperm (see Fig. 3B) and appearing as an oval, globular sac. Bursa copulatrix of ANC110092103 empty, flaccid and oblong. Shorter tube of vaginal bifurcation leading to junction of mucous gland duct (outward), prostate duct (central) and oviduct (inward). Mucous gland (Figs. 3A, 4B, 5C, 6B) transversally developed, compressed against pericardium. Mucous gland subdivided into two pouches disposed dorsally and ventrally to gland duct end.

Prostate (=prostate gland) (Figs. 3A, 4B,D, 5C, 6B-D) situated in between mucous gland and bursa copulatrix. Prostate bigger than mucous gland. Prostate external wall strongly folded showing several ridges. Prostatic internal epithelium easily distinguishable from thin and smooth epithelium of mucous gland.

Vas deferens beginning at junction of oviduct with prostate and mucous glands ducts. Vas deferens (Figs. 3A,B, 6A-D) running backwards above vaginal duct, then penetrating body wall and going forward over ciliated groove. Vas deferens lumen very reduced.

Oviduct (Figs. 3B, 5C) running backwards through prostate gland posterior folds, then compressing against albumen gland. Albumen gland (Figs. 3A,B, 4A,B,D, 5A-D, 6A,B) massive occupying most of visceral cavity posterior half. Albumen gland internally compact and externally smooth, although showing some peripheral folds. Albumen gland subdivided into two main lobes: one developed forward reaching body centre, the other one located caudo-dorsally overlying reproductive system. Albumen gland ducts not observed. Oviduct very flattened at junction of two lobes. Oviduct epithelium hardly distinguishable there, possibly fused to albumen gland walls. Oviduct strongly bent forward beyond this region leading into a digitiform seminal receptacle (Fig. 6D). Hermaphroditic duct opening ventrally at this area. In ANC110092104, hermaphroditic duct proximal part surrounded by a globous, thin-walled sac (=fertilization chamber; Fig. 6D). Hermaphroditic duct not coiled, running forwards until level of bursa copulatrix. and then folding backwards and joining to small ducts of three follicles of hermaphroditic gland (Figs. 3B, 4A,B, 5D, 6B). Hermaphroditic gland very compressed in ANC110092104, number of follicles not distinguishable. Hermaphroditic gland at left hind side of visceral cavity.

Reproductive system: anterior parts

Male genital opening (Fig. 2E) on oral lobe right side leading to a wide, cylindrical penial sheath (Figs. 3A, 6B). Penial insertion at cavity end. Penis diameter not exceeding half of penial sheath. Penis long, apparently smooth, armature not observed. Penial sheath diameter markedly reduced at level of half buccal mass, then running backwards joining with retractor muscle. Retractor muscle (Figs. 3A, 6B-D) self-curled at proximal part. Retractor muscle ventrally developed, ending at beginning of body posterior third, between pericardium and centre of bursa copulatrix.

Vas deferens leaving body wall underneath penial sheath. Vas deferens curving back and forth three or five times before entering penial sheath, near penial insertion. At this area, penial sheath inner wall defining a small penial papilla. Penial gland and solid concretions not observed over penial sheath.

DISCUSSION

The usefulness of micro-CT in the study of both external and internal anatomy of marine molluscs has been widely demonstrated (GOLDING & JONES, 2007; ALBA-TERCEDOR & SÁNCHEZ-TOCINO, 2011; FAULWETTER *et al.*, 2013; CANDÁS *et al.*, 2014, 2016, 2018; ZIEGLER *et al.*, 2018; MARCONDES MACHADO *et al.*, 2019; MARTÍNEZ-SANJUÁN *et al.*, 2022). Among Eupulmonata, micro-CT has been used for morphological shell studies of terrestrial snails (JOCHUM *et al.*, 2015, 2017, 2018, 2019; DE WINTER & DE GIER, 2019; INÄBIT *et al.*, 2019; JOCHUM *et al.*, 2020) but soft tissues have never been neither imaged nor described by this technique. Regarding Onchidiidae, micro-CT had only been applied once for the description of *Peronia persiae* MANIEI, ESPELAND, MOHAVEDI & WÄGELE, 2020 (MANIEI *et al.*, 2020). However, it was used as an accessorial technique alongside histology and dissection and no iconography was provided to assess its efficacy on anatomical studies in onchidiid slugs (MANIEI *et al.*, 2020).

In the present work, a detailed description of the external and internal anatomy of *Onchidella celtica* is given by using micro-CT. Furthermore, our descriptions are supported by high-quality images of 3D models as well as a 3D reconstruction of internal anatomy. Our results are discussed below compared to those descriptions found in the literature.

External morphology

The external morphology of *Onchidella celtica* is well known (DELLE CHIAJE, 1841-1844; PHILLIPPI, 1844; JOYEUX-LAFFUIE, 1882; MARCUS, 1979; CHEMELLO Y D'ANNA, 1986; TWEEN, 1987; WEISS & WÄGELE, 1998; BARILLÉ-BOYER *et al.*, 2000; GROH, 2006); our observations fairly agree with the previous aforementioned work. The length of the studied specimens matches with those from Great Britain (TWEEN, 1987), France (MARCUS, 1979; BARILLÉ-BOYER *et al.*, 2000) and Morocco (MARCUS, 1979). In addition, the maximum length of 25 mm recorded is twice that reported previously for this species in Galician waters (ROLÁN *et al.*, 1989; TRONCOSO & URGORRI, 1990).

According to DAYRAT *et al.* (2011b), the maximum length could vary between species, but the rest of external characters are affected by fixation and preservation processes and show great intra-specifically variation. Therefore, detailed measurements or length and width ratios, as well as colour or appearance of notum, are not appropriate to differentiate species of *Onchidella* (MARCUS, 1979; DAYRAT *et al.*, 2011b). This difficulty in distinguishing species by external features is widespread in most genera of the family, as almost all of them have externally cryptic species (DAYRAT *et al.*, 2017; GOULDING *et al.*, 2018a, 2018b; DAYRAT *et al.*, 2020). However, the sharpness of the notal structures in the scanned specimens is remarkable when compared to light microscopy or SEM examination (BARILLÉ-BOYER *et al.*, 2000; XU *et al.*, 2018).

Subdermal structures and glands

Subepidermal silicate spicules were described by LABBÉ (1933, 1934) below the notum and hyponotum of several onchidiids thus resulting in the erection of the order Silicodermatae; these findings were, however, refuted by several authors (see MARCUS, 1979). Spicule networks have been successfully studied with micro-CT in nudibranchs (ALBA-TERCEDOR & SÁNCHEZ-TOCINO, 2011; PENNEY *et al.*, 2018; PAZ-SEDANO et al., 2021; URGORRI *et al.*, 2021). Due to the preference of iodine for polysaccharides and calcified structures, hard tissues show

Nova Acta Científica Compostelana, 30 (2023). ISSN-e: 2340-0021
https://doi.org/10.15304/nacc.id8975

an excess in the brightness of micro-CT images. Consequently, spicule networks are more suitable for visualisation in unstained samples (ALBA-TERCEDOR & SÁNCHEZ-TOCINO, 2011; GIGNAC *et al*., 2016; CANDÁS *et al*., 2018). In the present work, no evidence of spicule or any other hardened subdermal deposits was found in ANC110092103. Thus, biosilification in Onchidiidae still remains unproven (DAYRAT, 2009; EHRLICH, 2019).

MARCUS (1979) emphasized the importance of the histochemistry and structure of perinotal glands to identify species of *Onchidella*. Histochemistry cannot be assessed by micro-CT, but this technique still allowed for a clear visualisation of its structure and disposition below the notum (see Fig. 5E). Our results are in line with those depicted in JOYEUX-LAFFUIE (1882), BINOT (1965) and MARCUS (1979) for *O. celtica* showing the outlet of the narrow glandular duct at the tip of perinotal papillae. Regarding its number, almost all authors agreed that this species possesses 10 pairs of glands in both Mediterranean (DELLE CHIAJE, 1841-1844; PHILLIPPI, 1844; CHEMELLO & D'ANNA, 1986) and Atlantic populations (JOYEUX-LAFFUIE, 1882; BINOT, 1965; MARCUS, 1979). However, WEISS & WÄGELE (1998) also described 8-9 pairs of glands in *O. celtica* thus highlighting intra-specific variability as it occurs in other *Onchidella* species (WATSON, 1925; MARCUS, 1978, 1979; DAYRAT *et al*., 2011b; GOULDING *et al*., 2022). On the other hand, histology and morphology of the pedal gland of *O. celtica* has been described (VAILLANT, 1872; JOYEUX-LAFFUIE, 1882; FRETTER, 1943; BINOT, 1965; WEISS & WÄGELE, 1998); our results mostly agree with previous work except for FRETTER (1943) who described a medial septum internally dividing the gland, not found in our examinations.

Digestive system

The presence of an inconspicuous jaw-like structure within the lips of the scanned specimens has been found as in other *Onchidella* species, including *O. celtica* (JOYEUX-LAFFUIE, 1882; VON WISSEL, 1904; WATSON, 1925; DAYRAT *et al*., 2011b). The radula has correctly been located within the buccal mass, but the shape and number of teeth could not be determined. Failure in distinguishing radular teeth by micro-CT has already been pointed out previously (CANDÁS *et al*., 2018; MARTÍNEZ-SANJUÁN *et al*., 2022). Nonetheless, ZIEGLER *et al*. (2018) noted that if the size of the radula is substantial, very high-quality images can be achieved with this technique. In Onchidiidae, while the radular formula seems to have a low reliability for species delimitation due to its high intra-specific variability (MARCUS, 1979; BRITTON, 1984), the shape of teeth usually helps at the genus level when observed with SEM (DAYRAT *et al*., 2011b, 2017, 2018, 2019a). Further studies will determine the effectiveness of Micro-CT against SEM for the visualisation of this trait.

The stomach of Onchidiidae exhibits a marked regionalisation which is better appreciated when it is full (FRETTER, 1943). Here, we have clearly observed the four chambers described in most *Onchidella* species (WATSON, 1925; FRETTER, 1943; TWEEN, 1987; WEISS & WÄGELE, 1998; DAYRAT *et al*., 2011). The smaller one (=stomach IV) has been clearly seen with micro-CT but is usually omitted in some descriptions and merely termed as "intestinal caecum" (JOYEUX-LAFFUIE, 1882; CHEMELLO & D'ANNA, 1986). The sizes of the chambers, the whole stomach and the digestive gland strongly vary between individuals (DAYRAT *et al*., 2011b). Thus, providing detailed measurements of each organ seems useless for taxonomic purposes (MARCUS, 1979).

According to the dorsal pattern of the intestine, PLATE (1893) distinguished four types of intestinal loops (types I-IV) in Onchidiidae, to which a fifth one (type V) was later added by LABBÉ (1934). Almost all onchidiid genera possess one or two types of intestinal loops and,

despite some intra-specific variation within a particular genus, nearly all species are characterised by a single intestinal type (DAYRAT *et al*., 2019b). The taxonomic value of this character for genera delimitation has recently been emphasized in the phylogeny of the family (GOULDING *et al*., 2022). The intestinal U-shaped loop of the scanned specimens (see Fig. 6C) fits with type IV, which is the only one present in the genus *Onchidella* (BRITTON, 1984; DAYRAT *et al*., 2011b; GOULDING *et al*., 2022).

Nervous system

The structure of the nervous system of Onchidiidae is essentially identical in all species (WATSON *et al*., 1925). The morphology and location of all ganglia has been clearly observed in the scanned specimens. The position of the visceral ganglia shows a high variability within *O. celtica* and *O. borealis*, i.e. displaced to the right (JOYEUX & LAFFUIE, 1882; WEISS & WÄGELE, 1998; this work) whereas other work reported them near to the left pleural ganglion (PLATE, 1893; VON WISSEL, 1898; STANTSCHINSKY, 1907); therefore, this character seems lacking taxonomic relevance (WEISS & WÄGELE, 1998). Regarding the nerves, WEISS & WÄGELE (1998) described 14 pedal nerves arising from pedal ganglia, while only 9 were observed in the scanned animals. The applied resolution was probably not sufficient to distinguish pairs of overlapping nerves (CANDÁS *et al*., 2018; MARTÍNEZ-SANJUÁN *et al*., 2022).

However, lower numbers of pedal nerves have been found in other *Onchidella* species (WATSON, 1925).

Circulatory system and renal-pulmonary comple

Detailed descriptions of the circulatory system were provided by VAILLANT (1872) and JOYEUX-LAFFUIE (1882). Our results did not show any relevant differences in comparison to previous work. Within the genus *Onchidella*, the position of pericardium constrains the right lung and kidney branches causing an asymmetrical course of both organs (WATSON, 1925). In *O. celtica*, the right branch is always longer than the left one (JOYEUX-LAFFUIE, 1882; FRETTER, 1943; WEISS & WÄGELE, 1998), whereas in other genera it may be the opposite or simply have a symmetrical development (BRITTON, 1984). As for the inner epithelium of the kidney, three different types were recognized by PLATE (1893) in *Onchidella*: lamellate, folded and smooth. The last one is present in *O. celtica* (WEISS & WÄGELE, 1998) and was also found in the scanned specimens. The observation of the renal-pulmonary complex by using micro-CT is noteworthy, since these organs are often overlooked due to its thin and inconspicuous epithelium (XU *et al*., 2018).

Reproductive system

The female reproductive parts of Onchidiidae are not relevant for species identification owing to their great variation in size and shape, which depends on the maturity and sexual activity of animals (BRITTON, 1984; DAYRAT *et al*., 2011b). However, some features observed here deserve to be commented when compared to previous descriptions of *O. celtica*. The presence of a fertilization chamber at the end of the hermaphroditic duct had only been quoted twice (FRETTER, 1943; CHEMELLO & D'ANNA, 1986). As for the mucous and prostate glands, most authors refer to them as "female mass gland" because they are difficult to distinguish from each other (WATSON, 1925; DAYRAT *et al*., 2011b). Indeed, it is often identified as "mucous

Nova Acta Científica Compostelana, 30 (2023). ISSN-e: 2340-0021
https://doi.org/10.15304/nacc.id8975

gland" (JOYEUX-LAFFUIE, 1882; WEISS & WÄGELE, 1998). In this work, clear visualisation of the inner epithelium of both glands was achieved by micro-CT. Our descriptions are consistent with those of VAILLANT (1872), FRETTER (1943) and CHEMELLO & D'ANNA (1986). Moreover, the vaginal gland was clearly observed and reconstructed. The presence of this structure in *O. celtica* has been reported by most authors apart from VAILLANT (1872) and WEISS & WÄGELE (1998). According to DAYRAT *et al.* (2011b), the vaginal gland is found only in *Onchidella* and *Hoffmannola* STRAND, 1932 and its opening at the end of the vaginal tube seems to vary between the two genera.

Regarding the male reproductive organs, BRITTON (1984) states that "these are the most widely used and trustworthy characteristics both at generic and specific level". The position of the male opening has been proposed as a reliable feature for supra-specific classification (HOFFMANN, 1928). However, there are many different interpretations in published work that often lead to misunderstandings (DAYRAT *et al.*, 2011b). In Onchidiidae, the absence or presence of the penial gland is usually a shared character within nearly all the species of the genus (see GOULDING *et al.*, 2022). The same occurs with the penial hooks, that could vary inter-specifically (GOULDING *et al.*, 2018b). *Onchidella* lacks both features as confirmed again in the scanned specimens. Hence, we cannot elucidate whether the use of micro-CT is appropriate for its observation in other onchidiids.

At the specific level, the length and coiling of the vas deferens has been proposed for species delineation (DAYRAT *et al.*, 2011b). Our results are in line with previous descriptions in *O. celtica* (SEMPER, 1885; MARCUS, 1979; CHEMELLO & D'ANNA, 1986; WEISS & WÄGELE, 1998). A small penial papilla was clearly seen in the scanned specimens near the attachment of the vas deferens to the penial sheath. This structure has already been described in *O. celtica* (JOYEUX-LAFFUIE, 1882; SEMPER, 1885; HOFFMAN, 1928; MARCUS, 1979) and is often absent in some species of the genus (MARCUS, 1979; DAYRAT *et al.*, 2011b). The presence of penial concretions has been mentioned in several species of *Onchidella* including *O. celtica* (JOYEUX-LAFFUIE, 1882; WATSON, 1925) but they were not observed in any of the scanned animals including the unstained specimen.

PLATE (1893) classified the attachment of the retractor muscle of onchidiids into three types: Type I (near the central nerve ring), Type II (close to the pericardium) and Type III (at the hind end of the visceral cavity). In the studied specimens, the end of the retractor muscle has been clearly observed at the level of the pericardium (see Fig. 6B) corresponding to Type II as previously reported for *O. celtica* (JOYEUX-LAFFUIE, 1882; HOFFMAN, 1928). Nonetheless, most previous work described it as a Type III (FRETTER, 1943; MARCUS, 1979; CHEMELLO & D'ANNA, 1986; WEISS & WÄGELE, 1998). Even though MARCUS (1979) and DAYRAT *et al.* (2011b) stressed the taxonomic importance of this character at the specific level, the variation of the attachment in individuals of the same species has also been found in *O. indolens* (Couthouy, 1852) (WEISS & WÄGELE, 1998). This trait has been well observed by means of micro-CT; therefore, its application to a larger number of specimens could assess whether shows variation and its potential taxonomic relevance.

Conclusions

The phylogenetic relationships of Onchidiidae have been reconstructed very recently considering molecular markers (GOULDING *et al.*, 2022). Except for *Onchidella*, the systematics of all genera of the family have been revised in the last few years from an integrative approach (see above). Therefore, an anatomical revision of all species of *Onchidella* seems necessary to clarify the aforementioned results.

Here, despite limitations restricted to the radula, the internal anatomy of *Onchidella celtica* has been successfully observed and reconstructed by using micro-CT. Futhermore, our observations are strongly in line with previous descriptions. Therefore, micro-CT is a very useful technique for a relatively rapid and non-destructive study of the internal anatomy of Onchidiidae. As this first approach has focused on a single species, future studies including other onchidiid genera will provide more consistent data to support our observations.

REFERENCES

ALBA-TERCEDOR, J., & SÁNCHEZ-TOCINO, L. (2011). The use of the SkyScan 1172 high-resolution micro-CT to elucidate if the spicules of the sea slugs (Mollusca: Nudibranchia, Opisthobranchia) have a structural or a defensive function. *SkyScan Users Meeting, 2011*, 113-121.

BARILLÉ-BOYER, A. L., GRUET, Y., PÉRUSSON, O., & BARILLÉ, L. (2000). Écologie et distribution du mollusque gastropode *Onchidella celtica* (Cuvier, 1817) sur l'estran rocheux de la Pointe de Saint-Gildas (Loire-Atlantique, France). *Bulletinde la Société des sciences naturelles de l'Ouest de la France, 22*(3), 123-138.

BINOT, D. (1965). Histologie, histochimie, cytologie de quelques formations glandulaires du tégument d'*Oncidiella celtica* (Cuv.) (Gastéropode Pulmoné). *Cahiers de Biologie Marine, 6*, 325-346.

BRITTON, K. M. (1984). The Onchidiacea (Gastropoda, Pulmonata) of Hong Kong with a worldwide review of the genera. *Journal of Molluscan Studies, 50*(3), 179-191. https://doi.org/10.1093/oxfordjournals.mollus.a065863

CANDÁS, M., DÍAZ-AGRAS, G., & URGORRI, V. (2014). The use of micro-CT for the study of the internal anatomy of sea slugs (Opisthobranchia, Nudibranchia, Dotidae). *SkyScan Users Meeting, 2014*, 241-243.

CANDÁS, M., DÍAZ-AGRAS, G., ABAD, M., BARRIO, L., CUNHA, X., PEDROUZO, L., SEÑARÍS, M. P., GARCÍA-ÁLVAREZ, Ó., & URGORRI, V. (2016). Application of micro-CT in the study of the anatomy of small marine molluscs. *Microscopy and Analysis, 30*(2), S8-S11.

CANDÁS, M., DÍAZ-AGRAS, G., GARCÍA-ÁLVAREZ, Ó., & URGORRI, V. (2018). Study of the applicability of micro-CT for identification of Mollusca Solenogastres. In *Proceedings of the Bruker Micro-CT User Meeting Abstract Book* (pp. 32-40).

CHEMELLO, R., & D'ANNA, G. (1986). Studio preliminare di una popolazione mediterranea di *Onchidella celtica* (Cuvier, 1817) (Mollusca: Onchidiida). *Lavori Società Italiana di Malacologia, 22*, 133-144.

DAYRAT, B. (2009). Review of the current knowledge of the systematics of Onchidiidae (Mollusca: Gastropoda: Pulmonata) with a checklist of nominal species. *Zootaxa, 2068*(1), 1-26. https://doi.org/10.11646/zootaxa.2068.1.1

DAYRAT, B. (2010). Anatomical re-description of the terrestrial onchidiid slug *Semperoncis montana* (Plate, 1893). *Malacologia, 52*(1), 1-20. https://doi.org/10.4002/040.052.0101

DAYRAT, B., & GOULDING, T. C. (2017). Systematics of the onchidiid slug *Onchidina australis* (Mollusca: Gastropoda: Pulmonata). *Archiv für Molluskenkunde, 146*(1), 121-133. https://doi.org/10.1127/arch.moll/146/121-133

DAYRAT, B., CONRAD, M., BALAYAN, S., WHITE, T. R., ALBRECHT, C., GOLDING, R., GOMES, S. R., HARASEWYCH, M. G. & DE FRIAS MARTINS, A. M. (2011a). Phylogenetic relationships and evolution of pulmonate gastropods (Mollusca): new insights from increased taxon sampling. *Molecular phylogenetics and evolution, 59*(2), 425-437. https://doi.org/10.1016/j.ympev.2011.02.014

DAYRAT, B., GOULDING, T. C., APTE, D., ASLAM, S., BOURKE, A., COMENDADOR, J., KHALIL, M., XUÂN, Q. N., TAN, S. H., & TAN, S. H. (2020). Systematic revision of the genus *Peronia* Fleming, 1822 (Gastropoda, Euthyneura, Pulmonata, Onchidiidae). *ZooKeys, 972*, 1-224. https://doi.org/10.3897/zookeys.972.52853

DAYRAT, B., GOULDING, T. C., APTE, D., BHAVE, V., COMENDADOR, J., QUA, N. X., TAN, S. K., & TAN, S. H. (2016). Integrative taxonomy of the genus *Onchidium* Buchannan, 1800 (Mollusca, Gastropoda, Pulmonata, Onchidiidae). *ZooKeys, 636*, 1-40. https://doi.org/10.3897/zookeys.636.8879

DAYRAT, B., GOULDING, T. C., BOURKE, A. J., KHALIL, M., & TAN, S. H. (2019a). New species and new records of *Melayonchis* slugs (Gastropoda: Euthyneura: Pulmonata: Onchidiidae). *Raffles Bulletin of Zoology, 67*, 557-585. https://doi.org/10.26107/RBZ-2019-0043

DAYRAT, B., GOULDING, T. C., KHALIL, M., APTE, D., & TAN, S. H. (2019c). A new species and new records of *Onchidium* slugs (Gastropoda, Euthyneura, Pulmonata, Onchidiidae) in South-East Asia. *ZooKeys, 892*, 27-58. https://doi.org/10.3897/zookeys.892.39524

DAYRAT, B., GOULDING, T. C., KHALIL, M., COMENDADOR, J., XUÂN, Q. N., TAN, S. K., & TAN, S. H. (2019b). A new genus of air-breathing marine slugs from South-East Asia (Gastropoda, Pulmonata, Onchidiidae). *ZooKeys, 877*, 31-80. https://doi.org/10.3897/zookeys.877.36698

DAYRAT, B., GOULDING, T. C., KHALIL, M., DEEPAK, A., BOURKE, A. J., COMENDADOR, J., & TAN, S. (2019d). A new genus and three new species of mangrove slugs from the Indo-West Pacific (Mollusca: Gastropoda: Euthyneura: Onchidiidae). *European Journal of Taxonomy, 500*, 1-77. https://doi.org/10.5852/ejt.2019.500

DAYRAT, B., GOULDING, T. C., KHALIL, M., LOZOUET, P., & TAN, S. H. (2018). Systematic revision one clade at a time: A new genus of onchidiid slugs from the Indo-West Pacific (Gastropoda: Euthyneura: Pulmonata). *Raffles Bulletin of Zoology, 66*, 814-837.

DAYRAT, B., ZIMMERMANN, S., & RAPOSA, M. (2011b). Taxonomic revision of the Onchidiidae (Mollusca: Gastropoda: Pulmonata) from the Tropical Eastern Pacific. *Journal of Natural History, 45*(15-16), 939-1003. https://doi.org/10.1080/00222933.2010.545486

DE WINTER, A. J., & DE GIER, W. (2019). A new Nigerian hunter snail species related to *Enneaserrata* d'Ailly, 1896 (Gastropoda, Pulmonata, Streptaxidae) with notes on the West African species attributed to Parennea Pilsbry, 1919. *ZooKeys, 840*, 21-34. https://doi.org/10.3897/zookeys.840.33878

DELLE CHIAJE, S. (1841-1844). Descrizione e notomia degli animali invertebrati della Sicilia citeriore osservati vivi negli anni 1822-1830. Parts 1-8. Batteli & Co., Naples.

EHRLICH, H. (2019). Spicular structures in Molluscs. In *Marine Biological Materials of Invertebrate Origin* (pp. 133-157). Springer, Cham. https://doi.org/10.1007/978-3-319-92483-0_10

FAULWETTER, S., DAILIANIS, T., VASILEIADOU, A., & ARVANITIDIS, C. (2013). Contrast enhancing techniques for the application of micro-CT in marine biodiversity studies. *Microscopy and analysis, 27*(2), S4-S7.

FRETTER, V. (1943). Studies in the functional morphology and embryology of *Onchidella celtica* (Forbes and Hanley) and their bearing on its relationships. *Journal of the Marine Biological Association of the United Kingdom, 25*(4), 685-720. https://doi.org/10.1017/S0025315400012467

GIGNAC, P.M., KLEY, N.J., CLARKE, J.A., COLBERT, M.W., MORHARDT, A.C., CERIO, D., COST, I.N., COX, P.G., DAZA, J.D., EARLY, C.M., ECHOLS, M.S., HENKELMAN, R.M., HERDINA, A.N., HOLLIDAY, C.M., LI, Z., MAHLOW, K., MERCHANT, S., MÜLLER, J., ORSBON, C.P., PALUH, D.J., THIES, M.L., TSAI, H.P., & WITMER, L.M. (2016). Diffusible iodine-based contrast-enhanced computed tomography (diceCT): an emerging tool for rapid, high-resolution, 3-D imaging of metazoan soft tissues. *Journal of Anatomy, 228*, 889-909. https://doi.org/10.1111/joa.12449

GOLDING, R. E., & JONES, A. S. (2007). Micro-CT as a novel technique for 3D reconstruction of molluscan anatomy. *Molluscan Research, 27*(3), 123-128.

GOULDING, T. C., BOURKE, A. J., COMENDADOR, J., KHALIL, M., QUANG, N. X., TAN, S. H., TAN, S. K., & DAYRAT, B. (2021). Systematic revision of *Platevindex* Baker, 1938 (Gastropoda: Euthyneura: Onchidiidae). *European Journal of Taxonomy, 737*, 1-133. https://doi.org/10.5852/ejt.2021.737.1259

GOULDING, T. C., KHALIL, M., TAN, S. H., & DAYRAT, B. (2018a). A new genus and a new species of onchidiid slugs from eastern Indonesia (Gastropoda: Euthyneura: Onchidiidae). *Raffles Bulletin of Zoology, 66*, 337-349.

GOULDING, T. C., KHALIL, M., TAN, S. H., & DAYRAT, B. (2018a). Integrative taxonomy of a new and highly-diverse genus of onchidiid slugs from the Coral Triangle (Gastropoda, Pulmonata, Onchidiidae). *ZooKeys, 763*, 1-111. https://doi.org/10.3897/zookeys.763.21252

GOULDING, T. C., KHALIL, M., TAN, S. H., CUMMING, R. A., & DAYRAT, B. (2022). Global diversification and evolutionary history of onchidiid slugs (Gastropoda, Pulmonata). *Molecular Phylogenetics and Evolution, 168*, 107360. https://doi.org/10.1016/j.ympev.2021.107360

GOULDING, T. C., TAN, S. H., TAN, S. K., APTE, D., BHAVE, V., NARAYANA, S., SALUNKHE, R., & DAYRAT, B. (2018b). A revision of *Peronina* Plate, 1893 (Gastropoda: Euthyneura: Onchidiidae) based on mitochondrial and nuclear DNA sequences, morphology and natural history. *Invertebrate Systematics, 32*(4), 803-826. https://doi.org/10.1071/IS17094

HOFFMANN, K. (1928) Zur Kenntniss der Oncidiiden. Ein Beitrag zur geographischen Verbreitung, Phylogenie und Systematik dieser Tiere. I. Teil. Untersuchung neuen Materials und Revision der Familie. *Zoologische Jahrbücher, Systematik Ökologie und Geographie der Tiere*, 55, 29-118.

INÄBNIT, T., JOCHUM, A., KAMPSCHULTE, M., MARTELS, G., RUTHENSTEINER, B., SLAPNIK, R., NESSELHAUF, C., & NEUBERT, E. (2019). An integrative taxonomic study reveals carychiid microsnails of the troglobitic genus *Zospeum* in the Eastern and Dinaric Alps (Gastropoda, Ellobioidea, Carychiinae). *Organisms Diversity & Evolution,* 19, 135-177. https://doi.org/10.1007/s13127-019-00400-8

JOCHUM, A., PRIETO, C. E., KAMPSCHULTE, M., MARTELS, G., RUTHENSTEINER, B., VRABEC, M., DÖRGE, D. D., & DE WINTER, A. J. (2019). Re-evaluation of *Zospeum schaufussi* von Frauenfeld, 1862 and *Z. suarezi* Gittenberger, 1980, including the description of two new Iberian species using Computer Tomography (CT) (Eupulmonata, Ellobioidea, Carychiidae). *Zookeys, 4*(835), 65-86. https://doi.org/10.3897/zookeys.835.33231

JOCHUM, A., RUTHENSTEINER, B., KAMPSCHULTE, M., MARTELS, G., KNEUBÜHLER, J., & FAVRE, A. (2018). Fulfilling the taxonomic consequence after DNA Barcoding: *Carychium panamaense* sp. n. (Eupulmonata, Ellobioidea, Carychiidae) from Panama is described using computed tomographic (CT) imaging. *ZooKeys*, 795, 1-12. https://doi.org/10.3897%2Fzookeys.795.29339

JOCHUM, A., WEIGAND, A. M., BOCHUD, E., INÄBNIT, T., DÖRGE, D.D., RUTHENSTEINER, B., FAVRE, A., MARTELS, G., & KAMPSCHULTE, M. (2017). Three new species of *Carychium* O.F. Müller, 1773 from the Southeastern USA, Belize and Panama are described using computer tomography (CT) (Eupulmonata, Ellobioidea, Carychiidae). *Zookeys*, 675, 97-127. https://doi.org/10.3897/zookeys.675.12453

JOYEUX-LAFFUIE, J. (1882). *Organisation et développement de l'Oncidie, Oncidium celticum cuv*. A. Hennuyer.

KEKLIKOGLOU, K., FAULWETTER, S., CHATZINIKOLAOU, E., WILS, P., BRECKO, J., KVAČEK, J., METSCHER, B., & ARVANITIDIS, C. (2019). Micro-computed tomography for natural history specimens: a handbook of best practice protocols. *European Journal of Taxonomy, 522*, 1-55. https://doi.org/10.5852/ejt.2019.522

LABBÉ, A. (1933). Les Oncidiadés, Mollusques à silice. *Notes des Comptes-Rendus de l'Académie des Sciences, 197*, 697-699.

LABBÉ, A. (1934). Opisthobranches et Silicodermés (Oncidiadés). *Résultats scientifiques du Voyage aux Indes Orientales Néerlandaises, 2*(14), 3-83, pl. I.

MANIEI, F., ESPELAND, M., MOVAHEDI, M., & WAEGELE, H. (2020). Description of a new *Peronia* species (Gastropoda: Eupulmonata: Onchidiidae) from Iran, Persian Gulf. *Zootaxa, 4758*(3), 501-531. https://doi.org/10.11646/zootaxa.4758.3.5

MARCONDES MACHADO, F., PASSOS, F. D., & GIRIBET, G. (2019). The use of micro-computed tomography as a minimally invasive tool for anatomical study of bivalves (Mollusca: Bivalvia). *Zoological Journal of the Linnean Society, 186*(1), 46-75. https://doi.org/10.1093/zoolinnean/zly054

MARCUS, E. D. B. R. (1978). The western Atlantic species of *Onchidella* (Pulmonata). *Sarsia, 63*(4), 221-224. https://doi.org/10.1080/00364827.1978.10411343

MARCUS, E. D. B. R. (1979). The Atlantic species of *Onchidella* (Gastropoda Pulmonata) part 2. *Boletim de Zoologia, São Paulo, 4*, 1-38.

MARTÍNEZ-SANJUÁN, J., KOCOT, K., GARCÍA-ÁLVAREZ, Ó., CANDÁS, M., & DÍAZ-AGRAS, G. (2022). Computed Microtomography (Micro-CT) in the Anatomical Study and Identification of Solenogastres (Mollusca). *Frontiers in Marine Science*, 8, 760194. https://doi.org/10.3389/fmars.2021.760194

PARAPAR, J., CANDÁS, M., CUNHA-VEIRA, X., & MOREIRA, J. (2017). Exploring annelid anatomy using micro-computed tomography: A taxonomic approach. *Zoologischer Anzeiger, 270*, 19-42. https://doi.org/10.1016/j.jcz.2017.09.001

PAZ-SEDANO, S., CANDÁS, M., GOSLINER, T. M., & POLA, M. (2021). Undressing *Lophodoris danielsseni* (Friele & Hansen, 1878) (Nudibranchia: Goniodorididae). *Organisms Diversity & Evolution, 21*(1), 107-117. https://doi.org/10.1007/s13127-020-00470-z

PENNEY, B. K., EHRESMANN, K. R., JORDAN, K. J., & RUFO, G. (2020). Micro-computed tomography of spicule networks in three genera of dorid sea-slugs (Gastropoda: Nudipleura: Doridina) shows patterns of phylogenetic significance. *Acta Zoologica, 101*(1), 5-23. https://doi.org/10.1111/azo.12266

PHILIPPI, R.A. (1841). Zoologische Bemerkungen. *Archiv für Naturgeschichte, Berlin, 7*(1), 42-59.

PLATE, L. VON (1893) Studien über opisthopneumone Lungeschnecken, II, Die Oncidiidien. *Zoologische Jahrbücher, Anatomie und Ontogenie der Thiere*, 7, 93-234.

ROLÁN, E., SCHMITT, J. O., & ÁLVAREZ, E. R. (1989). *Moluscos de la Ría de Vigo: Poliplacoforos, bivalvos, escafopodos, cefalopodos*. Universidade de Santiago de Compostela, Servizo de publicacións e intercambio científico.

SEMPER C. 1885. Dritte familie, Onchidiidae. In: Semper, C. (Ed.) *Reisen im Archipel der Philippinen, Wissenschaftliche Resultate*, III (7). Wiesbaden: C.W. Kreidel; pp. 251-290.

STANTSCHINSKY, W. (1907). Zur Anatomie und Systematik der Gattung *Oncidium*. Zoologische Jahrbücher, Systematik. *Geographie und Biologie der Tiere, 25*, 353-402.

TRONCOSO, J. S., & URGORRI, V. (1990). Nuevos datos sobre la distribución de seis especies de moluscos en las costas de Galicia. *Iberus, 9*(1-2), 247-252.

Tween T.C. (1987) *On the occurrence, ecology and behaviour of Onchidella celtica (Gastropoda, Onchidiacea) in the littoral of Cornwall*. PhD thesis. University of Bedfordshire, United Kingdom.

URGORRI, V. (1981). *Opistobranquiosde Galicia: estudio faunístico y zoográfico*. PhD thesis. University of Santiago de Compostela, Spain.

URGORRI, V., SEÑARÍS, M. P., AGRAS, G. J. D., CANDÁS, M., & RODRÍGUEZ, C. G. (2021). *Doris adrianae* sp. nov. (Heterobranchia; Nudibranchia; Doridina) from the Galician coasts (NW Iberian Peninsula). *Nova Acta Científica Compostelana (Bioloxía), 28*, 1-33. https://doi.org/10.15304/nacc.id7500

VAILLANT, M. L. (1872). Anatomico-zoological remarks upon *Oncidium celticum*, Cuvier. *Annals and Magazine of Natural History, 9*(49), 101-104.

VON WISSEL, K. (1898). Beiträge zur Anatomie der Gattung *Oncidiella*. Zoologische Jahrbücher, Suppl. 4: 583-640.

WATSON, H. (1925). The South African species of the molluscan genus *Onchidella*. *Annals of the South African Museum, 20*, 237-308.

WEISS, K., & WÄGELE, H. (1998). On the morphology, anatomy and histology of three species of *Onchidella* (Gastropoda: Gymnomorpha: Onchidiida). *Archiv für Molluskenkunde, 127*, 69-91. http://dx.doi.org/10.1127/arch.moll/127/1998/69

XU, G., YANG, T., WANG, D., LI, J., LIU, X., WU, X., & SHEN, H. (2018). A comprehensive comparison of four species of Onchidiidae provides insights on the morphological and molecular adaptations of invertebrates from shallow seas to wetlands. *Plos one, 13*(4), e0196252. https://doi.org/10.1371/journal.pone.0196252

ZIEGLER, A., BOCK, C., KETTEN, D. R., MAIR, R. W., MUELLER, S., NAGELMANN, N., PRACHT, E. D., & SCHRÖDER, L. (2018). Digital three-dimensional imaging techniques provide new analytical pathways for malacological research. *American Malacological Bulletin, 36*(2), 248-273. https://doi.org/10.4003/006.036.0205

Appendix

List of figures

Figure 1. *Onchidella celtica*. Habitus and external appearance *in vivo*. **A:** Dorsal view of a dark grey adult ANC207102102. **B:** Dorsal view of a green olive adult ANC202032101. **C:** Dorsal view of a whitish juvenile specimen ANC329032106. **D:** Ventral view of a light grey adult ANC217012102. **E:** Ventral view of a green olive adult ANC126022102.

Figure 2. Habitus and external appearance of the scanned specimens. **A:** Dorsal view of ANC110092104. **B:** Dorsal view of ANC110092103 stained. **C:** Dorsal view of ANC110092103 unstained. **D:** Ventral view of ANC110092104. **E:** Detail of the cephalic region of ANC110092104. **F:**Ventral view of ANC110092103 unstained. **G:** Detail of the caudal region of ANC110092103 stained.

Figure 3. A-B: Internal anatomy of ANC110092104 from right-sagittal view.

Figure 4. A: Internal anatomy of ANC110092104 from left-sagittal view. **B:** Internal anatomy of ANC110092103 unstained from left-sagittal view. **C:** Detail of the cephalic region of ANC110092103 unstained from right-sagittal view. **D:** Detail of the caudal region of ANC110092104 from left-sagittal view.

Figure 5. Internal anatomy of ANC110092104. **A-C:** Front-dorsal view. **D:** Front-ventral view. **E:** Transverse section of a perinotal gland showing the outlet of the glandular duct at the tip of the marginal papilla.

Figure 6: Internal anatomy of ANC110092104 reconstructed with Amira® v.5.4.4 software. **A:** Dorsal view. **B:** Ventral view. Central nervous ring containing cerebral ganglia (pink), pleural ganglia (blue), visceral ganglion (green) and pedal ganglia (yellow). (*) showing the end of the penial retractor muscle. **C:** Right lateral view (digestive and albumen glands transparent for better visualisation). **D:** Left lateral view (digestive and albumen glands transparent for better visualisation).

Abbreviations

a: anus	oe: oesophagus
ag: albumen gland	ol: oral lobe
ao: aorta	on: optical nerve
bb: buccal bulb	ot: optical tentacle
bc: bursa copulatrix	ov: oviduct
bg: buccal ganglia	pg: perinotal gland
cnr: central nervous ring	pn: pneumostome
dg: digestive gland	prg: prostatic gland
f: flagellum	ps: penial sheath
fo: female genital opening	rad: radula
hg: hermaphrodite gland	ras: radular sac
i: intestine	rm: retractor muscle
k: kidney	rsg: right salivary gland
l: lung	st I: stomach I
lsg: left salivary gland	st II: stomach II
m: mouth	st III: stomach III
mg: mucous gland	st IV: stomach IV
mo: male genital opening	v: vagina
mp: marginal papilla	vd: vas deferens
od: odontophore	

Nova Acta Científica Compostelana, 30 (2023). ISSN-e: 2340-0021
https://doi.org/10.15304/nacc.id8975